Equations for Cell Dynamics During 100% Effective Therapy. For therapy with RT inhibitors that are 100% effective ($e_r = 1$ for $t \geq 0$), analytical expressions can be derived from Eqs. **1**–**3** for T, $T^\star$, and $C^\star$ as a function of treatment time t. Relatively simple expressions for T can be found from Eq. **1** by focusing on the special cases $p = 0$ and $\lambda = 0$. If $p = 0$, we find

$$T(t) = T_0 e^{-\mu t} + (\lambda/\mu)(1 - e^{-\mu t}), \qquad [\mathbf{8}]$$

where T_0 is the value of T at $t = 0$. If $\lambda = 0$, we find

$$T(t) = \frac{(1 - \mu/p)T_c}{1 - [1 - (1 - \mu/p)T_c/T_0]e^{-(p-\mu)t}}. \qquad [\mathbf{9}]$$

When $p \neq 0$ and $\lambda \neq 0$,

$$T(t) = r_2 T_c + \frac{(r_1 - r_2)T_c}{1 - [1 - (r_1 - r_2)/(T_0/T_c - r_2)]\, e^{-p(r_1 - r_2)t}}, \qquad [\mathbf{10}]$$

where

$$r_{1,2} = \frac{1}{2}\left(\frac{p - \mu}{p}\right) \pm \frac{1}{2}\left[\left(\frac{p - \mu}{p}\right)^2 + \frac{4\lambda}{pT_c}\right]^{1/2}.$$

From Eqs. **2** and **3**, we find

$$T^\star(t) = T_0^\star e^{-\delta t} \qquad [\mathbf{11}]$$

and

$$C^\star(t) = C_0^\star e^{-\mu_C t}, \qquad [\mathbf{12}]$$

where $T_0^\star$ and $C_0^\star$ are the values of $T^\star$ and $C^\star$ at $t = 0$.

The Total Number of FDC Receptors and Characterization of the Pretreatment State of FDC Receptors and Viral Particles. We determine the fraction of receptors that are free, R/R_T, by numerically solving

$$1 = (R/R_T)\left[1 + (\alpha V_0/k_r)(1 + (R/R_T)(K_x R_T))^{n-1}\right], \qquad [\mathbf{13}]$$

which is derived from Eq. **7** and the steady-state forms of Eqs. **4** and **6**. We calculate the steady-state value of B_i/R_T for $i = 1, \ldots, n$ by using

$$B_i/R_T = \frac{1}{n} \begin{pmatrix} n \\ i \end{pmatrix} (\alpha V_0/k_r) \, (K_x R_T)^{i-1} (R/R_T)^i, \qquad [\mathbf{14}]$$

which is also derived from Eq. **7** and the steady-state forms of Eqs. **4** and **6**. We find R_T by using

$$R_T = F_0 / \left(\sum_{i=1}^{n} B_i/R_T \right), \qquad [\mathbf{15}]$$

which is derived from the identity $F_0 = \sum_{i=1}^{n} B_i$. These equations can be combined to determine the baseline values of R and each B_i.

Confidence limits on estimates of δ. Confidence limits, given in Tables 3 and 4, were calculated using a bootstrap method (1, 2). Best-fit parameter values were determined, as described in the main text, for each of 100 pairs of simulated data sets. Each simulated data set was generated by randomly drawing, M times, a data point from the corresponding set of M measurements. Recall that estimates of δ for triple therapy patients are derived from counts of infected mononuclear and $CD4^+$ T cells in lymphoid tissue (LT), whereas estimates of δ for ritonavir monotherapy patients are derived from plasma and tissue viral dynamics. The initial estimates of parameter values used to seed each fitting procedure were generated randomly. We only used estimates from procedures that converged to a reasonable fit, such that the sum of residuals was less than a fixed predetermined value. For each parameter, we sorted the 100 values obtained from bootstrapping in rank order. The 17th and 84th values, which are reported in Tables 3 and 4, define a 68% confidence interval.

Viral Dynamics. Plots similar to those in Fig. 2 of the main text are shown for each triple therapy patient in Fig. 5 and each monotherapy patient in Fig. 6. Plots similar to those in Fig. 3 of the main text, but on a shorter time scale, are shown for each monotherapy patient in Fig. 7. In each case of Fig. 7, a fraction of the virus

released from FDC, throughout treatment, is pretherapy virus (not shown after 10 d), but the fraction of pretherapy virus is typically less than that for a triple therapy patient.

Cellular Dynamics. Plots similar to those in Fig. 4 of the main text are shown for each triple therapy patient in Fig. 8.

References

1. Diaconis, P. & Efron, B. (1983) *Sci. Am.* **248**, 116–130.

2. Press, W. H., Teukolsky, S. A., Vetterling, W. T. & Flannery, B. P. (1992) *Numerical Recipes in FORTRAN: The Art of Scientific Computing* (Cambridge Univ. Press, Cambridge) 2nd Ed., pp. 686–687.

3. Notermans, D. W., Goudsmit, J., Danner, S. A., de Wolf, F., Perelson, A. S. & Mittler, J. (1998) *AIDS* **12**, 1483–1490.

4. Cavert, W., Notermans, D. W., Staskus, K., Wietgrefe, S. W., Zupancic, M., Gebhard, K., Henry, K., Zhang, Z.-Q., Mills, R., McDade, H., *et al.* (1997) *Science* **276**, 960–964.

5. Zhang, Z.-Q., Notermans, D. W., Sedgewick, G., Cavert, W., Wietgrefe, S., Zupancic, M., Gebhard, K., Henry, K., Boies, L., Chen, Z., *et al.* (1998) *Proc. Natl. Acad. Sci. USA* **95**, 1154–1159.

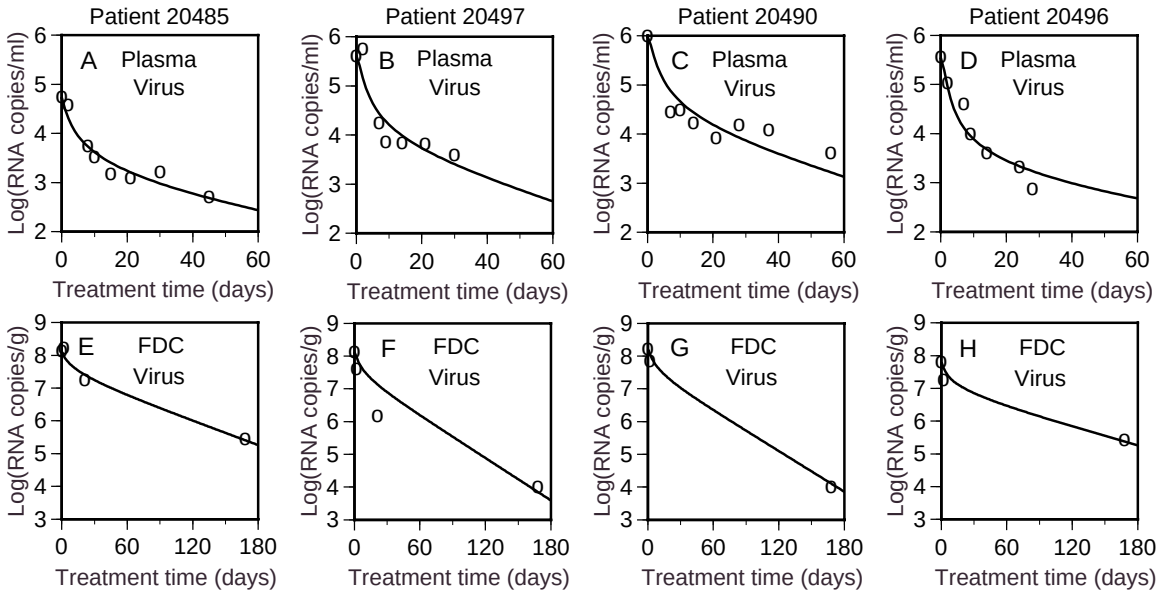

Fig. 5. Decay of free (*A*–*D*) and FDC-associated (*E*–*H*) virus in triple therapy patients 20485, 20497, 20490, and 20496. Points represent measurements of HIV-1 RNA per ml of plasma (3) or HIV-1 RNA per g of LT (4). Best-fit theoretical curves are derived by calculating $V + \hat{V}$ (upper) or $\sum_{i=1}^{n}(B_i + \hat{B}_i)$ (lower) as a function of treatment time t. Calculations are based on Eqs. **4**–**7** and parameter values in Tables 1 and 2.

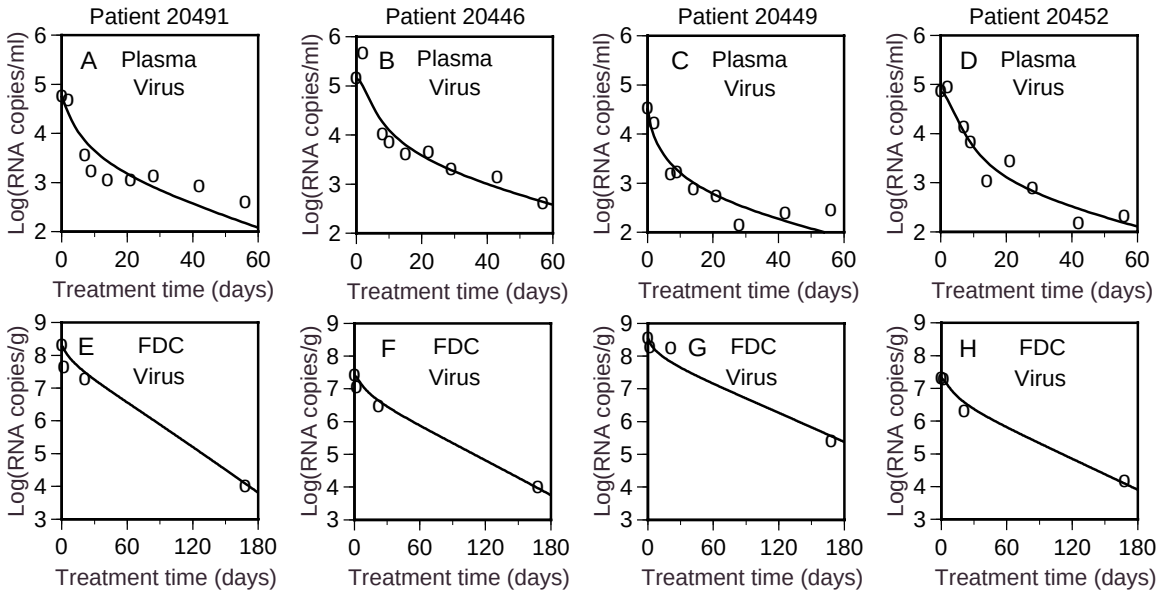

Fig. 6. Decay of free (*A*–*D*) and FDC-associated (*E*–*H*) virus in ritonavir monotherapy therapy patients 20491, 20446, 20449, and 20452. Points represent measurements of HIV-1 RNA per ml of plasma (3) or HIV-1 RNA per g of LT (4). Best-fit theoretical curves are derived by calculating $V + \hat{V}$ (upper) or $\sum_{i=1}^{n}(B_i + \hat{B}_i)$ (lower) as a function of treatment time t. Calculations are based on Eqs. **4**–**7** and parameter values in Tables 1 and 2.

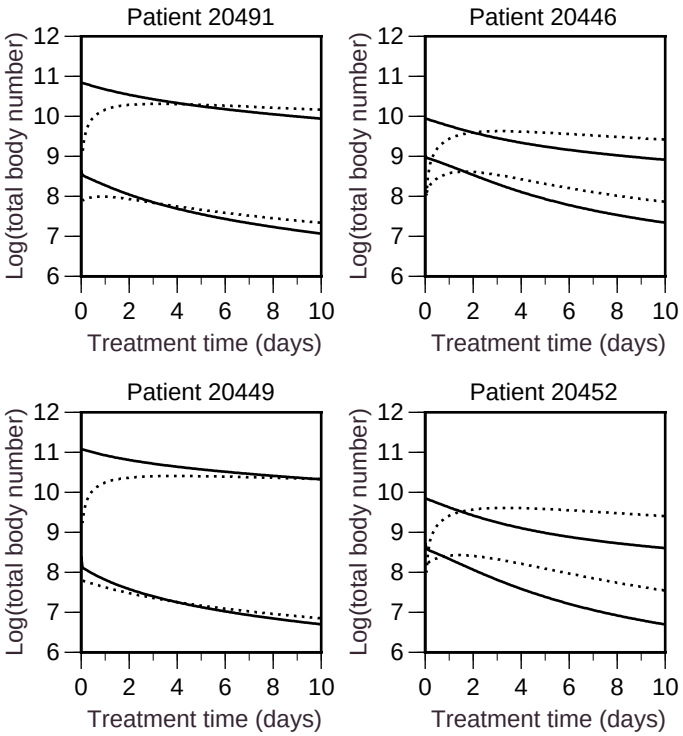

Fig. 7. The theoretical decay curves of Fig. 6 are replotted to show total body numbers of potentially infectious (solid lines) and noninfectious therapy-modified (dotted lines) viral particles that are associated with FDC in LT (upper) or free in extracellular fluid (lower).

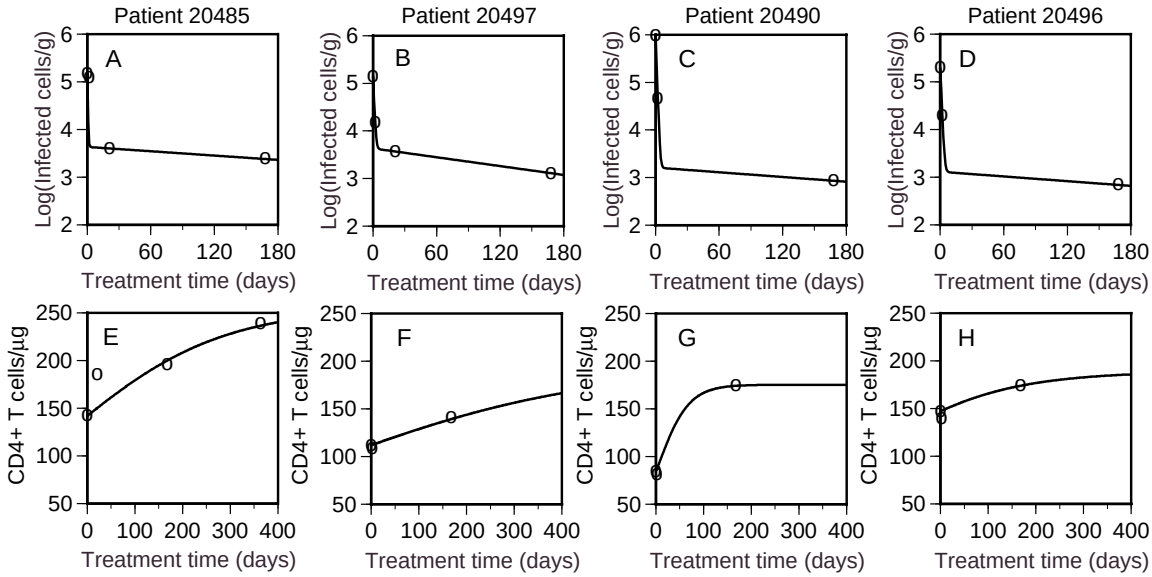

Fig. 8. Decay of infected cells (*A*–*D*) and recovery of target cells (*E*–*H*) in triple therapy patients 20485, 20497, 20490, and 20496. Points represent counts of infected mononuclear cells per g of LT (4) or $CD4^+$ T cells per μg of LT (5). Best-fit theoretical curves are derived by calculating $T^\star+C^\star$ (upper) or $T+T^\star+C^\star$ (lower) as a function of treatment time t. Calculations are based on Eqs. **1**–**3**, $\lambda = 0$ (all target cell expansion caused by proliferation), and parameter values in Tables 1 and 2.

Table 3. Confidence limits on estimates of δ, p, and T_c from cellular dynamics

	limits on δ (d^{-1})		limits on $p \times 100$ (d^{-1})		limits on $T_c \times 10^{-11}$	
Patient	lower	upper	limit	upper	lower	upper
20485	2.0	24	0.85	9.7	1.4	3.3
20497	1.2	1.4	0.55	0.89	2.1	23
20490	1.4	1.6	3.4	3.8	1.4	1.4
20496	0.93	1.2	0.56	1.1	2.0	12

Table 4. Confidence limits on estimates of δ, c, and $K_x R_T$ from viral dynamics

	limits on δ (d^{-1})		limits on c (d^{-1})		limits on $K_x R_T$	
Patient	lower	upper	limit	upper	lower	upper
20491	78	1200	73	110	0.89	0.98
20446	0.85	43	4.4	5.2	0.87	0.91
20449	1.1	52	370	530	1.0	1.1
20452	0.42	0.74	8.9	13	0.96	1.0